Heliyon 10 (2024) e34523

Contents lists available at ScienceDirect

Heliyon

journal homepage: www.cell.com/heliyon

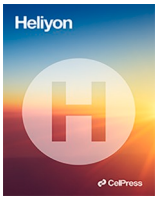

Research article

Integrative and comprehensive pan-cancer analysis of ubiquitin specific peptidase 11 (*USP11*) as a prognostic and immunological biomarker

Lijuan Cui *, Ling Yang, Boan Lai, Lingzhi Luo, Haoyue Deng, Zhongyi Chen, Zixing Wang

Pathology Department, Suining Central Hospital, Suining, Sichuan, 629000, China

ARTICLE INFO

Keywords:
USP11
Prognosis
Immunotherapy
Pan-cancer
Immune cell

ABSTRACT

The significance of *USP11* as a critical regulator in cancer has garnered substantial attention, primarily due to its catalytic activity as a deubiquitinating enzyme. Nonetheless, a thorough evaluation of *USP11* across various cancer types in pan-cancer studies remains absent. Our analysis integrates data from a variety of sources, including five immunotherapy cohorts, thirty-three cohorts from The Cancer Genome Atlas (TCGA), and sixteen cohorts from the Gene Expression Omnibus (GEO), two of which involve single-cell transcriptomic data. Our findings indicate that aberrant *USP11* expression is predictive of survival outcomes across various cancer types. The highest frequency of genomic alterations was observed in uterine corpus endometrial carcinoma (UCEC), with single-cell transcriptome analysis revealing significantly higher *USP11* expression in plasmacytoid dendritic cells and mast cells. Notably, *USP11* expression was associated with the infiltration levels of $CD8^+$ T cells and natural killer (NK) activated cells. Additionally, in the skin cutaneous melanoma (SKCM) phs000452 cohort, patients with higher *USP11* mRNA levels during immunotherapy experienced a significantly shorter median progression-free survival. *USP11* emerges as a promising molecular biomarker with significant potential for predicting patient prognosis and immunoreactivity across various cancer types.

1. Introduction

Ubiquitin-specific peptidase 11 (*USP11*), a prominent member of the largest subfamily of cysteine protease deubiquitinating enzymes, is integral to the regulation of various biological processes, including cell cycle control, DNA repair mechanisms, and tumor development. *USP11* is located in a gene cluster on chromosome Xp11 and comprises 23,963 amino acids, with an approximate molecular weight of 109,817 Da [1]. Like its counterparts USP4 and USP15, *USP11* features two ubiquitin-like (UBL) domains and an N-terminal domain specific to ubiquitin-specific proteases [2]. The N-terminal domain of *USP11* is particularly noteworthy for its critical cysteine residue at position 318, which is essential for its enzymatic activity. Mutations or deletions affecting this residue can lead to a loss of deubiquitinating function [3,4]. Unique to *USP11*, its UBL domain exhibits a tandem arrangement with a shortened β-hairpin at the interface of the two domains and distinct surface characteristics [3]. *USP11* primarily resides in the nucleus of non-dividing cells and is widely distributed throughout cells undergoing mitosis [1].

* Corresponding author. Pathology Department, Suining Central Hospital, Suining, Sichuan, 629000, China.
E-mail address: smileclj@126.com (L. Cui).

https://doi.org/10.1016/j.heliyon.2024.e34523
Received 3 February 2024; Received in revised form 2 July 2024; Accepted 10 July 2024
Available online 11 July 2024

USP11 exhibits a strong binding affinity towards several substrates, facilitating their stabilization and deubiquitination. One notable interaction involves RAN binding protein 9 (RANBP9), where *USP11* promotes the deubiquitination and subsequent stabilization of RANBP9, thereby correcting microtubule nucleation [1]. Recent investigations have also revealed *USP11*'s role in regulating the function of antigen-presenting cells in conjunction with v-rel reticuloendotheliosis viral oncogene homolog b (RELB) [5]. Additionally, *USP11* significantly influences various biological processes, including inflammation, immunity, cell proliferation, and apoptosis. For instance, it modulates TNFα-mediated NF-κB activation by stabilizing IκB kinase α (IKKα), thus exerting regulatory control over this signaling pathway [6]. Moreover, *USP11* enhances transforming growth factor β1 (TGFβ1) signaling by deubiquitinating and stabilizing TβRII, contributing to the regulation of cellular responses mediated by TGFβ1 [7]. *USP11* is also implicated in the regulation of the Hippo pathway through its modulation of the VGLL4/YAP-TEADs regulatory loop, indicating its involvement in controlling cell growth and organ size [8]. Collectively, these studies provide compelling evidence that *USP11* exerts its biological functions through interactions with multiple regulators, including RANBP9, RELB, IKKα, TGFβ1, and components of the Hippo pathway, among others.

In addition to its previously described roles, *USP11* is prominently involved in the regulation of DNA repair processes, which is of particular physiological importance. Recent studies have identified a novel binding site within the non-catalytic ubiquitin-like (UBL) region of *USP11*. Crystal structure analysis of the *USP11* peptide complex has demonstrated that this binding site interacts with a helical motif, thereby exerting regulatory control over *USP11*'s function in DNA repair processes [9]. *USP11* has emerged as a crucial regulator of the repair of double-strand breaks (DSBs), a significant type of DNA damage. Its interaction with BRCA2 has been identified as a key mechanism by which *USP11* regulates DSB repair [10]. Additionally, *USP11* is involved in the recruitment of specific DSB repair proteins, such as TP53BP1 and RAD51, to the sites of DNA damage, ensuring efficient repair [11]. Further evidence underscores *USP11*'s essential role in facilitating the efficient repair of DNA damage by homologous recombination proteins BRCA1 and BRCA2 [11].

In this study, we utilized data from both the TCGA project and GEO databases to conduct a comprehensive pan-cancer analysis of *USP11*. Our investigation encompassed an assessment of differential expression, correlations between *USP11* expression levels and patient survival, identification of associated microRNAs, evaluation of genetic alterations, and exploration of potential drugs and immune infiltration. Additionally, we examined the potential of *USP11* as a biomarker for immunotherapy, employing five real-world immunotherapy cohorts and two single-cell datasets. To our knowledge, this represents the first comprehensive analysis of the molecular mechanisms of *USP11* using multi-omics data and the first investigation of the association between *USP11* and immune response across various cancer types.

Table 1
List of cancer types.

Study Abbreviation	Study Name
ACC	Adrenocortical carcinoma
BLCA	Bladder Urothelial Carcinoma
BRCA	Breast invasive carcinoma
CESC	Cervical squamous cell carcinoma and endocervical adenocarcinoma
CHOL	Cholangiocarcinoma
COAD	Colon adenocarcinoma
DLBC	Lymphoid Neoplasm Diffuse Large B-cell Lymphoma
ESCA	Esophageal carcinoma
GBM	Glioblastoma multiforme
HNSC	Head and Neck squamous cell carcinoma
KICH	Kidney Chromophobe
KIRC	Kidney renal clear cell carcinoma
KIRP	Kidney renal papillary cell carcinoma
LAML	Acute Myeloid Leukemia
LGG	Brain Lower Grade Glioma
LIHC	Liver hepatocellular carcinoma
LUAD	Lung adenocarcinoma
LUSC	Lung squamous cell carcinoma
MESO	Mesothelioma
OV	Ovarian serous cystadenocarcinoma
PAAD	Pancreatic adenocarcinoma
PCPG	Pheochromocytoma and Paraganglioma
PRAD	Prostate adenocarcinoma
READ	Rectum adenocarcinoma
SARC	Sarcoma
SKCM	Skin Cutaneous Melanoma
STAD	Stomach adenocarcinoma
TGCT	Testicular Germ Cell Tumors
THCA	Thyroid carcinoma
THYM	Thymoma
UCEC	Uterine Corpus Endometrial Carcinoma
UCS	Uterine Carcinosarcoma
UVM	Uveal Melanoma

2. Materials and methods

2.1. Data acquisition

The thirty-three cancers of interest in this study, with their full names and abbreviations, are presented in Table 1. Transcriptomic (mRNA and microRNA), genomic, and clinical data for these thirty-three cancer types, involving 10,251 patients from TCGA, were downloaded from Xena Browser. Microarray datasets from GEO, including GSE13507, GSE41258, GSE90604, GSE31056, GSE36895, GSE11151, GSE101728, GSE10072, GSE30219, GSE71729, GSE87211, GSE15605, GSE46517, and GSE63678, which contain information on adjacent normal tissues, were also downloaded (https://www.ncbi.nlm.nih.gov/geo/) [12–24].

The results of the analysis of two single-cell datasets of primary uterine corpus endometrial carcinoma, GSE154763 (n = 9) and GSE139555 (n = 3), were accessed through the Tumor Immune Single-cell Hub 2 (TISCH2) online platform (http://tisch.comp-genomics.org/home/) to investigate the distribution of the *USP11* gene across cell subpopulations [25–27].

Data from two immunotherapy cohorts, specifically bladder urothelial carcinoma (BLCA, GSE176307) and skin cutaneous melanoma (SKCM, GSE100797), were sourced from the Gene Expression Omnibus (GEO) [28,29]. Information regarding two immunotherapy cohorts involving kidney renal clear cell carcinoma (KIRC) patients (PMID32472114 and PMID32895571) was gathered from supplementary literature, with the cohorts named after the PubMed identifiers of the respective studies [30,31]. The phs000452 cohort of SKCM was accessed from the Melanoma Genome Sequencing Project [32].

2.2. Survival analysis

In each cancer type, patients were evenly stratified into three groups based on their *USP11* expression, namely *USP11*-High, *USP11*-Middle, and *USP11*-Low. Cox proportional hazards survival analysis comparing the *USP11*-High and *USP11*-Low patient groups was conducted using the R package survival. The results were visualized using forest plots generated with the R package forestplot to illustrate the correlation [33,34]. Kaplan-Meier curves were generated using the R package survminer to compare the differences in survival times between these groups [35].

2.3. USP11-linked miRNA

The miRNA prediction for *USP11* was conducted using the R package multiMiR across six miRNA-mRNA interaction databases: ElMMo, MicroCosm, miRanda, DIANA-microT, PITA, and TargetScan [36]. The prediction results were visualized in the form of an upset map using the R package UpSetR to illustrate overlaps and unique predictions among databases [37]. Pearson correlation analysis between *USP11* expression and miRNA levels was performed using the R package Hmisc [38]. Heatmaps were generated with the R package pheatmap to display correlation patterns, while scatter plots and boxplots were created using the R package ggpubr [39,40].

2.4. Pathways enrichment analysis

In the TCGA datasets of UCEC or SKCM patients, individuals were evenly categorized into three groups based on their *USP11* expression levels: *USP11*-high, *USP11*-middle, and *USP11*-low. Differential gene expression analysis was performed using the R package "edgeR", applying a fold change threshold of ≥ 2 and an adjusted p-value of <0.05 [41]. Subsequently, KEGG and GO pathway enrichment analyses were conducted with the R package "clusterprofiler" using hypergeometric tests on the set of differentially expressed genes [42].

2.5. Drug sensitivity

The Genomics of Drug Sensitivity in Cancer (GDSC) version 2 database encompasses IC50 values and transcriptomic data from 167 drug-treated cell lines. Using the R package oncoPredict, IC50 values for each patient in the TCGA cohort are predicted based on their transcriptomic profiles [43]. To assess the relationship between IC50 values and *USP11* expression, Pearson correlation calculations were performed, followed by the creation of a heatmap, scatter plot, and box plot, following the methodology outlined in the *USP11*-linked miRNA section.

2.6. Immune infiltration

The CIBERSORT absolute algorithm was utilized to assess the extent of immune cell infiltration [44]. This calculation encompassed the evaluation of twenty-two immune cell scores obtained from TIMER2.0 [45]. For details on the calculation of Pearson correlation between IC50 and *USP11* expression, as well as the generation of heatmap and box plot visuals, please refer to the *USP11*-linked miRNA section of the method.

2.7. Statistical analysis

All statistical analyses were conducted using the R programming language (https://www.r-project.org/). Differences between two

groups and among multiple groups were assessed using Wilcoxon's test and one-way analysis of variance (ANOVA), respectively. Kaplan-Meier analysis and log-rank tests were employed to evaluate differences in overall survival between groups. A p-value <0.05 was considered statistically significant unless otherwise specified.

3. Results

3.1. Expression of USP11

A comprehensive gene expression analysis of *USP11* across various cancers was performed using data from the TCGA and GEO projects. The mRNA levels of *USP11* were notably higher in LGG and pheochromocytoma and paraganglioma (PCPG) (Fig. 1A). Significant variations in *USP11* transcriptional levels were observed between tumor tissues and adjacent normal tissues across sixteen cancer types, as illustrated in Fig. 1B. Comparative analysis indicated significantly reduced expression of *USP11* in BLCA, breast invasive carcinoma (BRCA), KIRC, kidney renal papillary cell carcinoma (KIRP), lung adenocarcinoma (LUAD), lung squamous cell carcinoma (LUSC), prostate adenocarcinoma (PRAD), thyroid carcinoma (THCA), and uterine corpus endometrial carcinoma (UCEC) compared to normal tissues. Conversely, elevated expression of *USP11* was detected in head and neck squamous cell carcinoma (HNSC), kidney chromophobe (KICH), and liver hepatocellular carcinoma (LIHC) (all p-values <0.05) relative to normal tissues. Analysis of GEO datasets further revealed significant downregulation of *USP11* in tumor tissues of KIRP, LUAD, LUSC, pancreatic adenocarcinoma (PAAD), and UCEC, while showing upregulation in normal tissues of rectum adenocarcinoma (READ) and skin cutaneous melanoma (SKCM) (Fig. 1C).

3.2. Prognostic biomarker

To evaluate the impact of *USP11* on cancer patient prognosis, we conducted a comprehensive analysis examining the relationship between *USP1*1 mRNA expression levels and survival outcomes. Patients from each cancer type were categorized into three groups

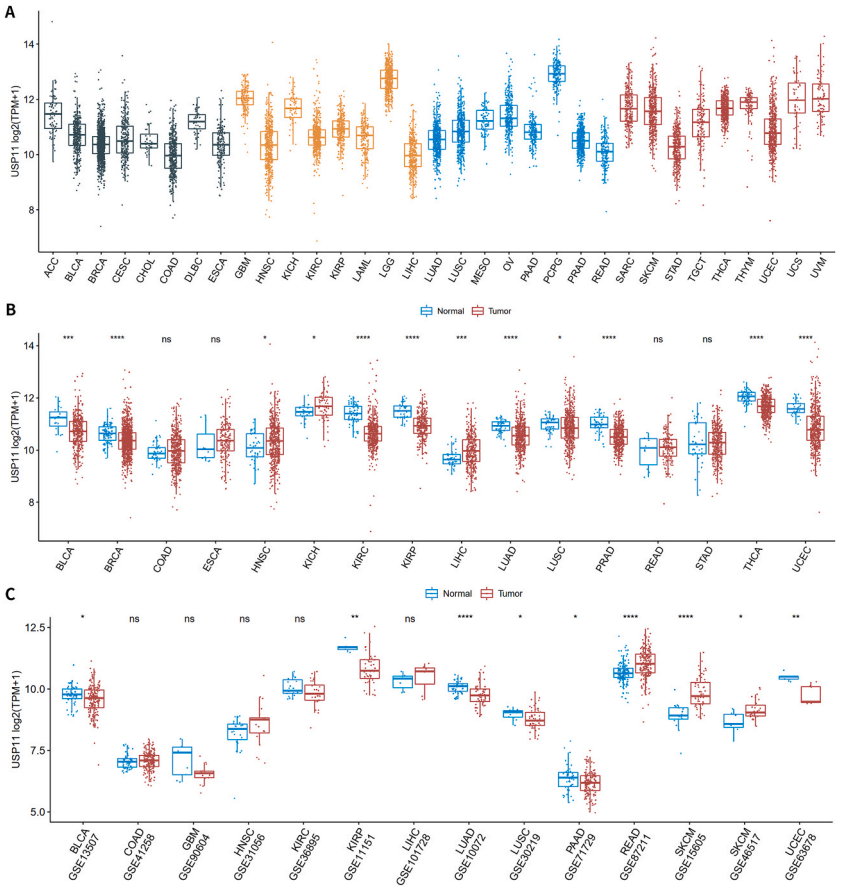

Fig. 1. The *USP11* expression status in different tumors and normal tissues. (A) The mRNA expression of *USP11* across thirty-three cancer types from TCGA data. **(B)** The TCGA project's *USP11* gene expression difference in sixteen different tumors and adjacent normal tissues. **(C)** The GEO project's *USP11* gene expression difference in fourteen different tumors and adjacent normal tissues.

based on *USP11* expression levels, and a forest plot was generated to visualize their associations with overall survival (OS). The findings revealed that high *USP11* expression was significantly correlated with improved overall survival in CESC, KICH, LGG, PAAD, and UVM (Fig. 2A). Further detailed analysis focusing on CESC demonstrated that patients with elevated *USP11* expression had prolonged overall survival (log-rank p for trend = 0.018; HR = 0.51, 95 % CI 0.29–0.90) (Fig. 2B). Similar Kaplan-Meier survival curves were observed for KICH (p = 0.048; HR = 0.16, 95 % CI 0.03–0.94), LGG (p < 0.001; HR = 0.38, 95 % CI 0.25–0.58), PAAD (p = 0.005; HR = 0.49, 95 % CI 0.30–0.80), and UVM (p = 0.010; HR = 0.26, 95 % CI 0.10–0.67) (Fig. 2C, D, 2E, and 2F).

3.3. Genetic alteration

To thoroughly explore the mutational profile of *USP11* in cancer progression, we conducted comprehensive analyses of mutations and copy number variations (CNVs) using genomic data sourced from the TCGA database across thirty-two different cancer types. Out of the 11,141 patients included in our study, 394 individuals exhibited *USP11* gene variants, among which 42 patients had both *USP11* mutations and CNVs (Fig. 3A). Comparative analyses with the remaining 10,705 patients without *USP11* variants (Fig. 3B, C, and 3D) revealed notable findings: patients with *USP11* mutations (255 patients) demonstrated a significantly more favorable overall survival prognosis (p = 0.034; HR = 0.79, 95 % CI 0.64–0.96), whereas those with *USP11* copy number amplifications (120 patients) exhibited poorer overall survival outcomes (p = 0.028; HR = 1.35, 95 % CI 0.99–1.83). However, there was no significant difference in overall survival observed among patients with *USP11* copy number deletions (61 patients). It is essential to acknowledge that due to varying

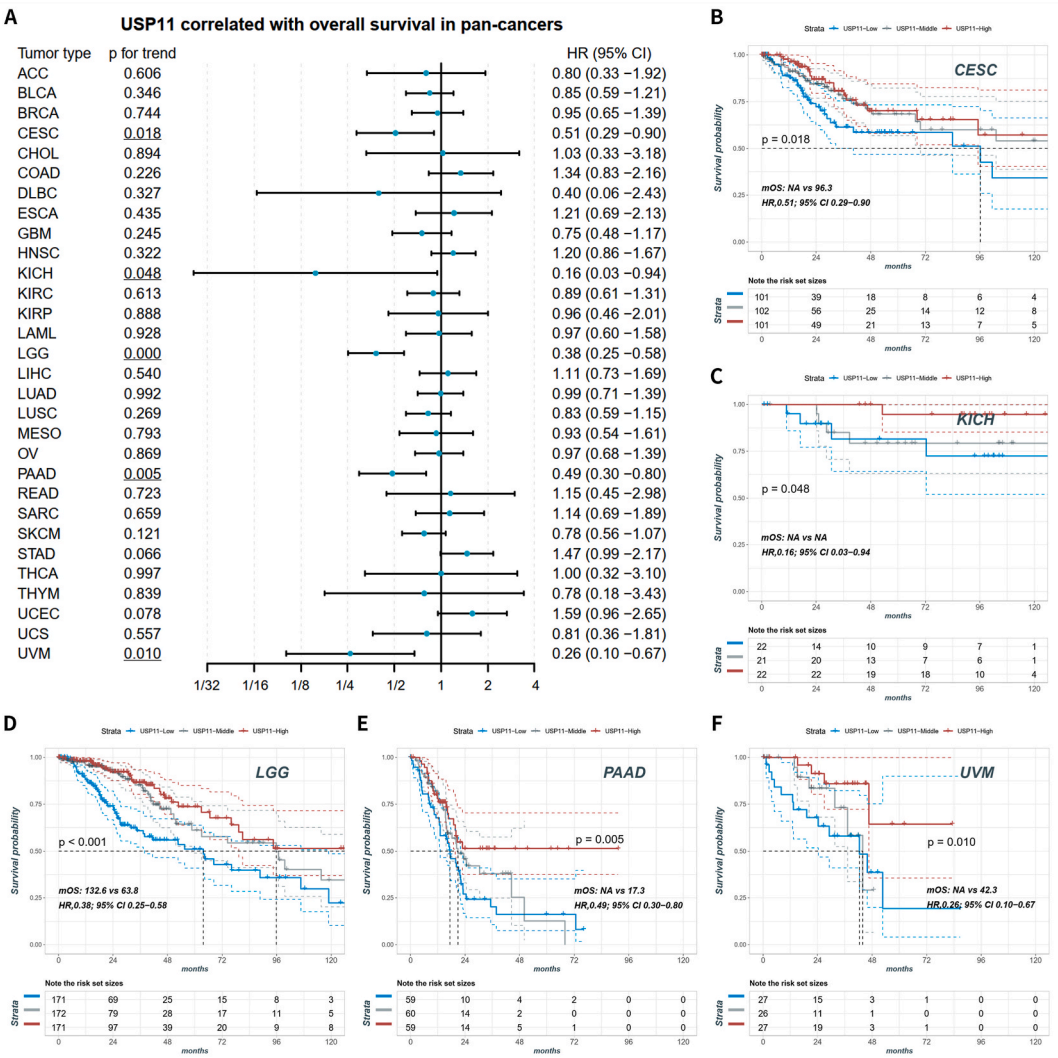

Fig. 2. Association of *USP11* with overall survival prognosis. (A) Hazard ratio of *USP11* expression in different cancers from the TCGA dataset. **(B–F)** Kaplan–Meier OS analysis of *USP11* in CESC, KICH, LGG, PAAD and UVM in TCGA. The tertile value of *USP11* in each tumor was considered as the cutoff value.

Fig. 3. Genetic alterations of *USP11* with implication in prognosis. (A) Number of patients with *USP11* variants, including mutation and copy number amplification or deep deletion, in thirty-two cancers from the TCGA dataset. **(B)** Kaplan–Meier OS analysis of all patients with *USP11* mutation and wild. **(C)** Kaplan–Meier OS analysis of all patients with *USP11* amplification and wild. **(D)** Kaplan–Meier OS analysis of all patients with *USP11* deep deletion and wild. **(E)** The percentage of USP11 mutation, copy number amplification, deep deletion and all variants in different cancers.

patient numbers across different cancer types in the TCGA dataset, we performed statistical analyses to determine gene variation rates within each cancer type. The top three cancer types exhibiting the highest rates of *USP11* gene variations were UCEC, OV, and SKCM (Fig. 3E). Specifically, UCEC showed the highest mutation rate, OV had the greatest incidence of copy number amplifications, and esophageal carcinoma (ESCA) had the highest rate of copy number deletions (Fig. 3E).

3.4. Single cell localization

We analyzed the cellular distribution of *USP11* using single-cell datasets GSE154763 and GSE139555 in UCEC. In the GSE154763 dataset, cells were classified into dendritic cells (DC), mast cells, mono/macro cells, and plasmacytoid dendritic cells (pDCs) (Fig. 4A). Similar to the expression pattern of GZMB, *USP11* exhibited significantly higher expression levels in pDCs (Fig. 4B and C). In contrast, *USP11* showed elevated expression in mast cells, which differed from the expression pattern of GZMB (Fig. 4D). Moreover, compared to its expression in normal tissues, *USP11* displayed significantly higher expression levels in pDC cells and mast cells in tumor tissues (Fig. 4E). In the GSE139555 dataset, the cellular categories included conventional $CD4^+$ T cells (CD4Tconv), $CD8^+$ T cells (CD8T), $CD8^+$ T exhausted cells (CD8Tex), fibroblasts, proliferating T cells (Tprolif), and T regulatory cells (Treg) (Fig. 4F). Unlike CD8A, which exhibited preferentially high expression in CD8T, CD8Tex, and Tprolif cells, *USP11* showed broad expression across nearly all cell types but at a low mRNA level (Fig. 4G and H).

3.5. Immune infiltration

To explore the potential association between *USP11* gene expression and immune cell infiltration across various cancers in TCGA, we utilized the CIBERSORT-ABS algorithm. Our analysis unveiled a significant positive correlation between *USP11* expression and the

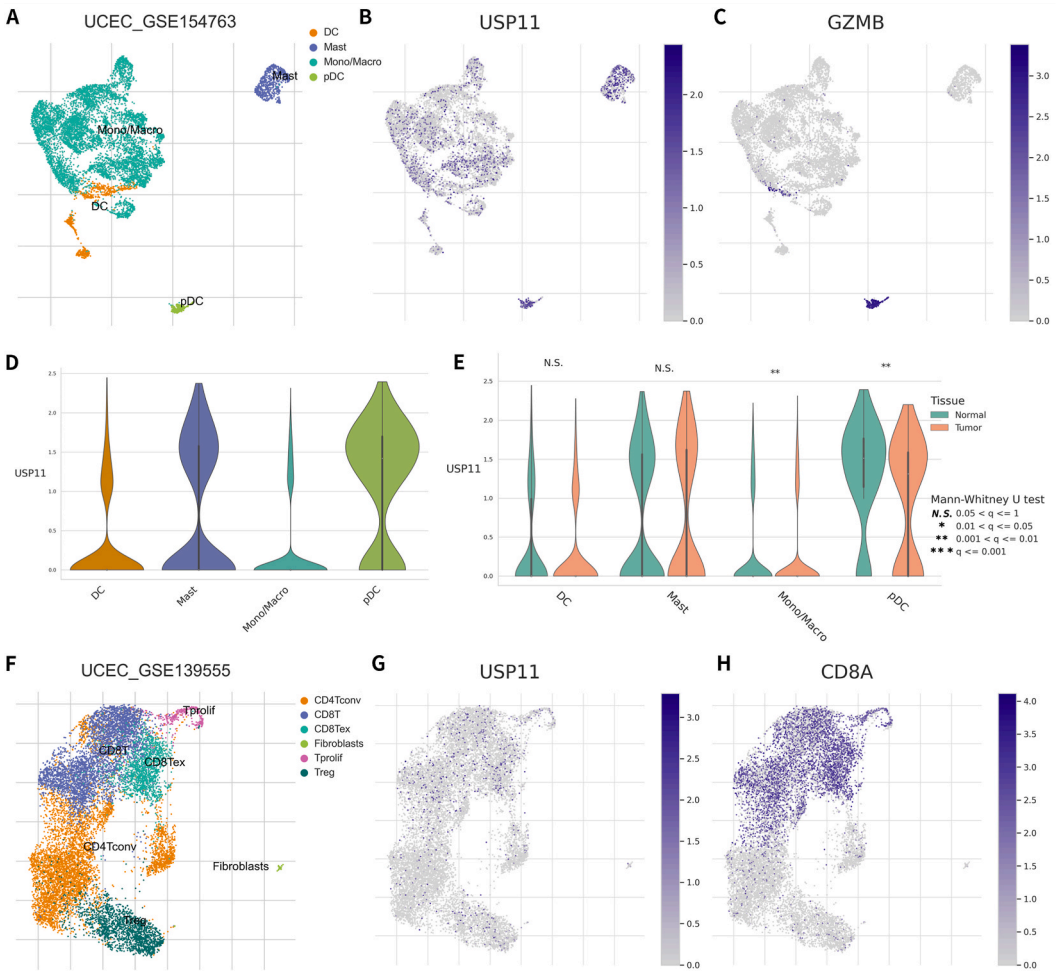

Fig. 4. Localizations of *USP11* in single cell level of UCEC datasets. (A) Cellular taxa of the GSE154763, including dendritic cells, mast cells, mono/macro cells, and plasmacytoid dendritic cells. (B) Distribution of *USP11*. (C) Distribution of *GZMB*. (D) Expression of *USP11* in tumor. (E) Comparisons of *USP11* in normal and tumor tissues. (F) Cellular taxa of the GSE139555, including CD4Tconv, CD8T, CD8Tex, fibroblasts, Tprolif, and Treg. (G) Distribution of *USP11*. (H) Distribution of *CD8A*.

infiltration of $CD8^+$ T cells and activated natural killer (NK) cells in ESCA, HNSC, LIHC, PRAD, and STAD tumors. Conversely, *USP11* expression showed a notable negative correlation with $CD8^+$ T cells and activated NK cells in LGG, THCA, and UVM tumors (Fig. 5A). Interestingly, in SKCM, a cancer type well-known for immunotherapy research, *USP11* demonstrated a significant positive correlation with resting NK cells and a negative correlation with M1 macrophages and resting mast cells (Fig. 5A). Moreover, in intergroup comparisons, we observed significantly higher infiltration of $CD8^+$ T cells in the *USP11* high expression group compared to the *USP11* low expression group in ESCA, HNSC, LIHC, PRAD, and STAD (Fig. 5B).

3.6. Biomarker for immunotherapy

To assess the potential of *USP11* as a biomarker for immunotherapy, we analyzed six real-world immunotherapy cohorts in this study. In the GSE176307 cohort of BLCA patients, those with high *USP11* expression showed a median progression-free survival (mPFS) of 2.2 months, which was better than the 1.4 months observed in subjects with low *USP11* expression. Although not reaching statistical significance, there was a trend towards improved outcomes in patients with high *USP11* expression (log-rank $p = 0.075$; HR = 0.52, 95 % CI 0.20–1.37) (Fig. 6A). However, in KIRC patients from the PMID32472114 and PMID32895571 cohorts, there was no significant difference in progression-free survival between the *USP11*-high and *USP11*-low groups following immunotherapy (Fig. 6B and C). In the SKCM phs000452 cohort, patients with higher *USP1*1 mRNA levels had significantly shorter PFS compared to patients with lower *USP1*1 mRNA levels (log-rank $p = 0.023$; mPFS: 2.8 months vs. 6.3 months; HR = 1.85, 95 % CI 1.04–3.63) (Fig. 6D). A similar trend was observed in the Kaplan-Meier survival curve of the GSE100797 cohort, another immunotherapy melanoma cohort, although the log-rank p-value did not reach statistical significance (Fig. 6E).

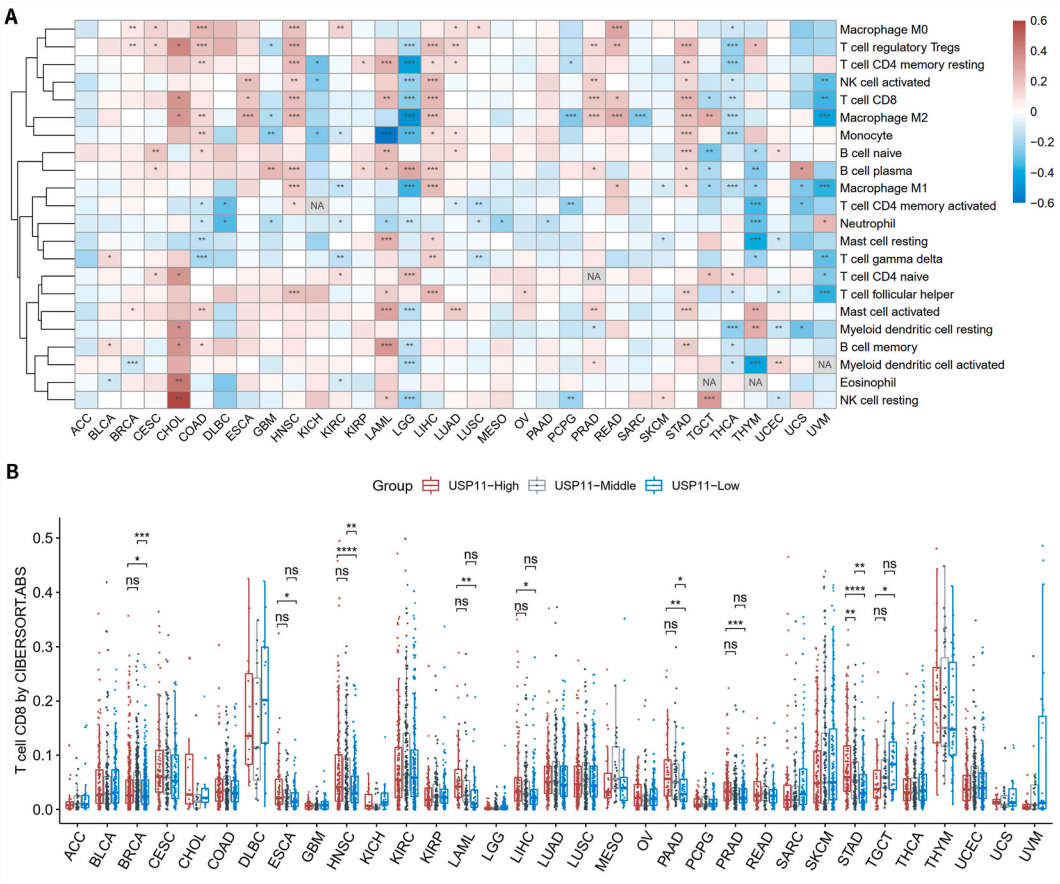

Fig. 5. ***USP11* in tumor immunity. (A)** Correlation of *USP11* expression with twenty-two immune infiltrating cells in pan-cancer by CIBERSORT Absolute algorithm. **(B)** Comparisons of $CD8^+$ T cell infiltration among *USP11* high, middle and low expression groups.

3.7. KEGG and GO pathways

Pathway enrichment analysis was conducted on differentially expressed genes between UCEC or SKCM patients with high and low *USP11* expression levels. In UCEC, 1619 genes were upregulated and 1485 genes were downregulated in the *USP11*-high group (Fig. 7A). A total of 31 KEGG pathways showed significant enhancement in UCEC patients with high *USP11* expression, including pathways like calcium signaling, cAMP signaling, and cytokine-cytokine receptor interaction (Fig. 7B). Additionally, 553 GO pathways were enriched in UCEC patients with high *USP11* expression (Supplementary Table 1, Sheet 1), and 202 GO pathways were enriched specifically (Fig. 7C and Supplementary Table 1, Sheet 2). In SKCM, 1147 genes were upregulated and 809 genes were downregulated in the *USP11*-high group (Fig. 7D). A total of 29 KEGG pathways were significantly enhanced in SKCM patients with high *USP11* expression, including pathways such as calcium signaling, cytokine-cytokine receptor interaction, and PI3K-Akt signaling (Fig. 7E). Moreover, 763 GO pathways were enriched in SKCM patients with high *USP11* expression (Supplementary Table 1, Sheet 3), and 225 GO pathways were enriched specifically (Fig. 7F and Supplementary Table 1, Sheet 4). Notably, 92 GO pathways were significantly enriched in both UCEC and SKCM patients with low *USP11* compared to those with high *USP11* (Fig. 7G and Supplementary Table 1, Sheet 5). Importantly, 23 of these 92 GO pathways were related to immune response, such as B cell activation, cell killing, humoral immune response, and immunoglobulin complex (Fig. 7H).

3.8. Potential drug

In the Genomics of Drug Sensitivity in Cancer (GDSC) version 2 database, transcriptomic data from 20 tumor cell lines were utilized following 161 drug treatments. Employing a ridge regression model, drug sensitivity across 20 cancer types was predicted for 8259 patients from TCGA, and its correlation with *USP11* expression levels was assessed (Fig. 8A). For each tumor type, two drugs exhibiting the strongest correlation with *USP11* expression were selected, resulting in a heatmap displaying 35 drugs based on their association with *USP11* (Fig. 8A). Among the findings, the most robust positive correlation was observed between UMI77 and *USP11* in LGG (Fig. 8B). Predicted IC50 values of UMI77 in BLCA, BRCA, HNSC, LGG, LIHC, PAAD, PRAD, STAD, THCA, and UCEC patients, stratified by *USP11* expression levels, showed notable differences between the groups (Fig. 8C). Conversely, the most substantial negative

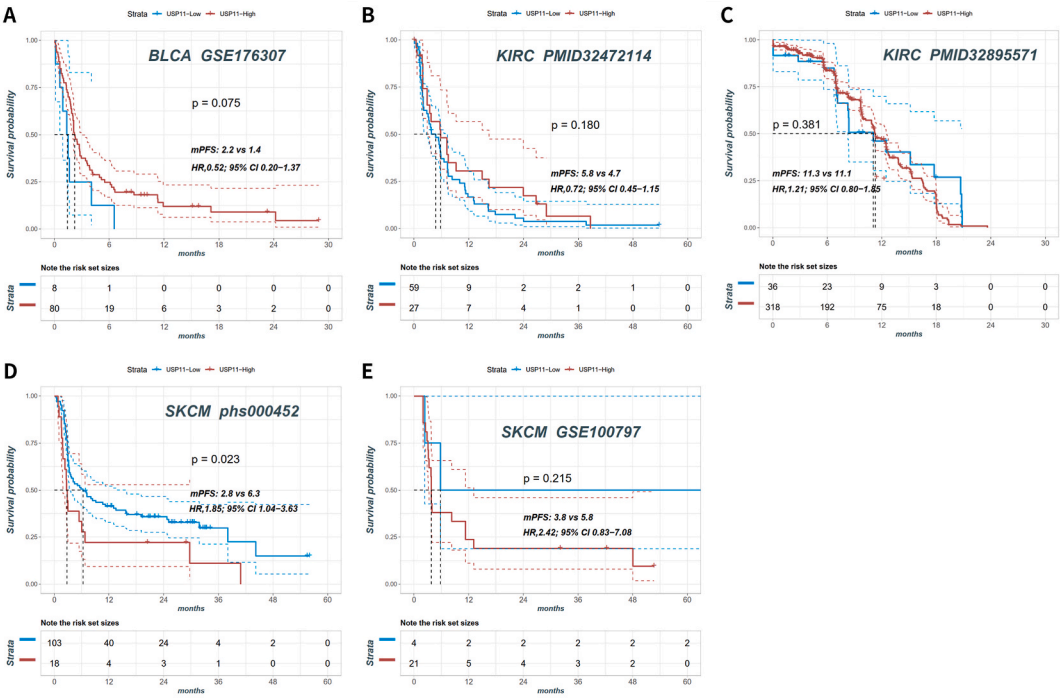

Fig. 6. *USP11* as biomarker in patients ongoing immunotherapy. Kaplan–Meier PFS analysis of USP11 in patients with BLCA from the GSE176307 cohort **(A)**, KIRC from the PMID32472114 cohort **(B)**, KIRC from the PMID32895571 cohort **(C)**, SKCM from the phs000452 cohort **(D)**, SKCM from the GSE100797 cohort **(E)**.

correlation was found between LY2109761 and *USP11* in LGG (Fig. 8D). Predicted IC50 values of LY2109761 in BRCA, CESC, DLBC, GBM, KIRC, PAAD, PRAD, SKCM, STAD, and UCEC patients, categorized by *USP11* expression, also demonstrated significant variations between the groups (Fig. 8E).

3.9. Targeted miRNA

MicroRNA interactions with *USP11* are pivotal in its regulatory mechanisms linked to physiological activities. Utilizing six databases, we identified a total of 186 potential microRNAs targeting *USP11* (Fig. 9A). Notably, TargetScan predicted 124 microRNAs, PITA identified 73, DIANA-microT found 48, MicroCosm detected 33, miRanda identified 21, and ElMMo pinpointed 10 microRNAs. Interestingly, 14 microRNAs were concurrently predicted by three or more of these databases (Fig. 9A). Subsequent analysis of TCGA pan-cancer project data revealed the presence of only 12 out of the 186 potential microRNAs targeting *USP11*. A heatmap depicting the correlation between these 12 microRNAs and *USP11* expression levels is shown (Fig. 9B). Notably, among these microRNAs, hsa.miR.199a.3p in PCPG (rho = −0.49, $p < 0.001$), hsa.miR.330.5p in KICH (rho = −0.46, $p < 0.001$), and hsa.miR125a.3p in TGCT (rho = −0.40, $p < 0.001$) exhibited the strongest negative correlations with *USP11* expression (Fig. 9C, D, 9E).

4. Discussion

USP11 has emerged as a pivotal regulator in numerous cancer-related signaling pathways, presenting promising avenues for targeted therapeutic strategies. Despite its recognized importance, our understanding of *USP11*'s role across various cancer types remains incomplete. To bridge this gap, our study adopted a comprehensive multiomics approach spanning thirty-three distinct cancer types. Our objective was to unravel the molecular mechanisms driving the heightened expression of *USP11* in cancer. Our findings not only underscore the prognostic relevance of *USP11* expression across diverse cancer types originating from various organs but also reveal its previously unrecognized crucial involvement in immune responses.

We have observed a widespread upregulation of *USP11* across diverse tumor types, underscoring its significant involvement in tumor progression. Through Cox proportional hazards model analysis and Kaplan-Meier survival curves in a pan-cancer study, we have established a notable correlation between increased *USP11* expression and enhanced overall survival in specific tumor types, namely CESC, KICH, LGG, PAAD, and UVM. These findings are substantiated by corroborative research from other scientific teams, affirming the prognostic relevance of *USP11* expression in cancer patients. For instance, in colorectal cancer research, the *USP11*/PPP1CA complex has been implicated in driving disease progression through the activation of the ERK/MAPK signaling pathway [46]. Investigations have also highlighted *USP11*'s upregulation in colorectal cancer, where it stabilizes IGF2BP3, thereby promoting proliferation and metastasis [47]. Moreover, the inhibition of *USP11* using mitoxantrone, a potential pancreatic cancer cell survival

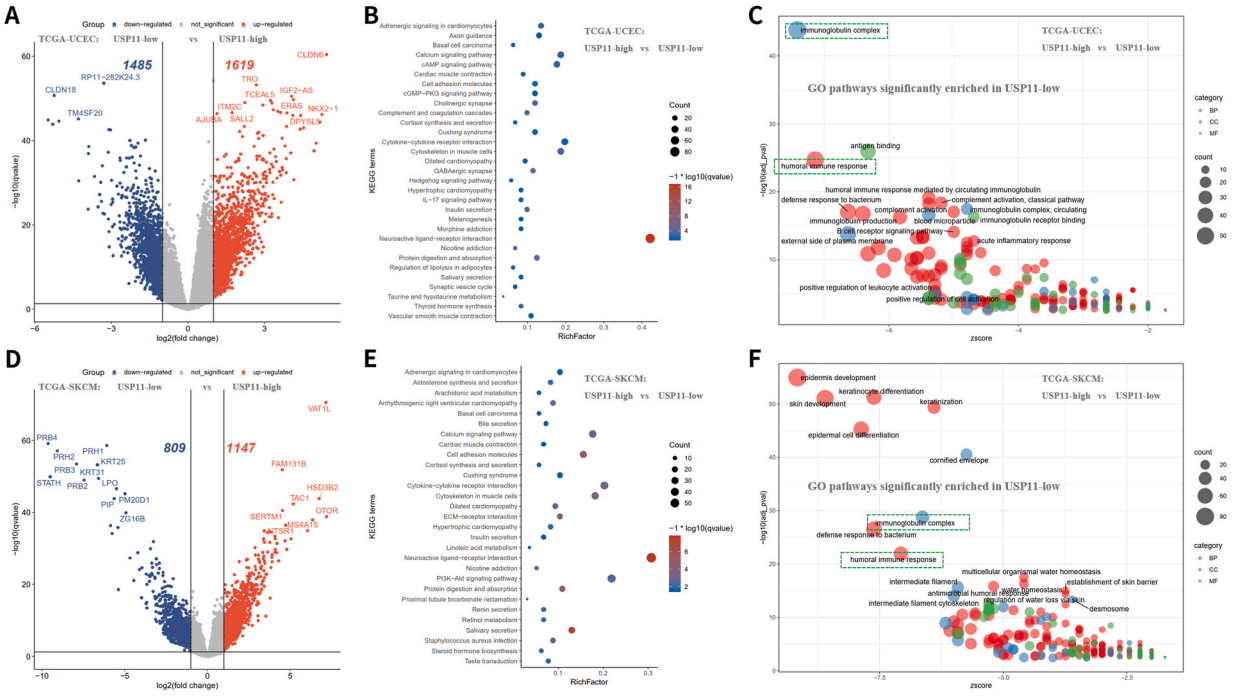

H 23 of 92 overlapped GO pathways were related to immune response

ID	Description	GO terms	q-value	Count	BgRatio
GO:0019814	immunoglobulin complex	CC	2.77E-27	44	167/19550
GO:0006959	humoral immune response	BP	5.73E-20	50	317/18723
GO:0050853	B cell receptor signaling pathway	BP	1.06E-09	23	131/18723
GO:0042571	immunoglobulin complex, circulating	CC	3.43E-09	17	77/19550
GO:0002440	production of molecular mediator of immune response	BP	6.40E-09	34	308/18723
GO:0002377	immunoglobulin production	BP	7.53E-09	28	216/18723
GO:0002455	humoral immune response mediated by circulating immunoglobulin	BP	5.22E-08	20	121/18723
GO:0034987	immunoglobulin receptor binding	MF	6.84E-08	16	79/18368
GO:0002443	leukocyte mediated immunity	BP	9.23E-06	35	440/18723
GO:0001906	cell killing	BP	1.40E-05	21	188/18723
GO:0016064	immunoglobulin mediated immune response	BP	1.60E-05	22	207/18723
GO:0019724	B cell mediated immunity	BP	2.01E-05	22	210/18723
GO:0050864	regulation of B cell activation	BP	2.98E-05	21	198/18723
GO:0002768	immune response-regulating cell surface receptor signaling pathway	BP	4.92E-05	27	315/18723
GO:0002449	lymphocyte mediated immunity	BP	1.08E-04	28	350/18723
GO:0002429	immune response-activating cell surface receptor signaling pathway	BP	1.08E-04	25	291/18723
GO:0002757	immune response-activating signal transduction	BP	1.08E-04	25	291/18723
GO:0050871	positive regulation of B cell activation	BP	1.48E-04	17	152/18723
GO:0002253	activation of immune response	BP	3.56E-04	28	375/18723
GO:0042113	B cell activation	BP	3.56E-04	26	334/18723
GO:0002764	immune response-regulating signaling pathway	BP	4.46E-04	32	468/18723
GO:0002696	positive regulation of leukocyte activation	BP	2.76E-02	24	409/18723
GO:0002920	regulation of humoral immune response	BP	4.47E-02	6	45/18723

Fig. 7. ***USP11*-related KEGG and GO enrichment analysis. (A)** Differently expressed genes in UCEC patients with *USP11*-high vs *USP11*-low. **(B)** KEGG pathways significantly enriched between UCEC patients with *USP11*-high and *USP11*-low. **(C)** GO pathways significantly enriched in UCEC patients with *USP11*-low. **(D)** Differently expressed genes in SKCM patients with *USP11*-high vs *USP11*-low. **(E)** KEGG pathways significantly enriched between SKCM patients with *USP11*-high and *USP11*-low. **(F)** GO pathways significantly enriched in SKCM patients with *USP11*-low. **(G)** The overlapped GO pathways enriched in UCEC and SKCM patients with *USP11*-low. **(H)** Immunity-related the overlapped GO pathways.

inhibitor, underscores its role in pancreatic cancer progression and therapeutic potential [48]. In breast cancer contexts, elevated *USP11* levels have been associated with increased invasiveness in vitro and enhanced metastatic potential in vivo experiments [49]. Interestingly, a cohort study involving breast cancer patients has revealed a significant association between high *USP11* expression and reduced survival rates [50]. Importantly, in hepatocellular carcinoma, *USP11* has emerged as a prognostic indicator of poor outcomes, facilitating metastasis through its deubiquitinating activity on NF90 [51,52]. Furthermore, *USP11* has been implicated in melanoma proliferation by deubiquitinating NONO, a protein upregulated in melanoma and associated with unfavorable prognoses [53]. Together, these findings underscore the therapeutic promise of targeting *USP11* across various malignancies, presenting new avenues for clinical interventions.

The infiltration of immune cells represents a prominent characteristic across various cancer types. While the specific role of *USP11*

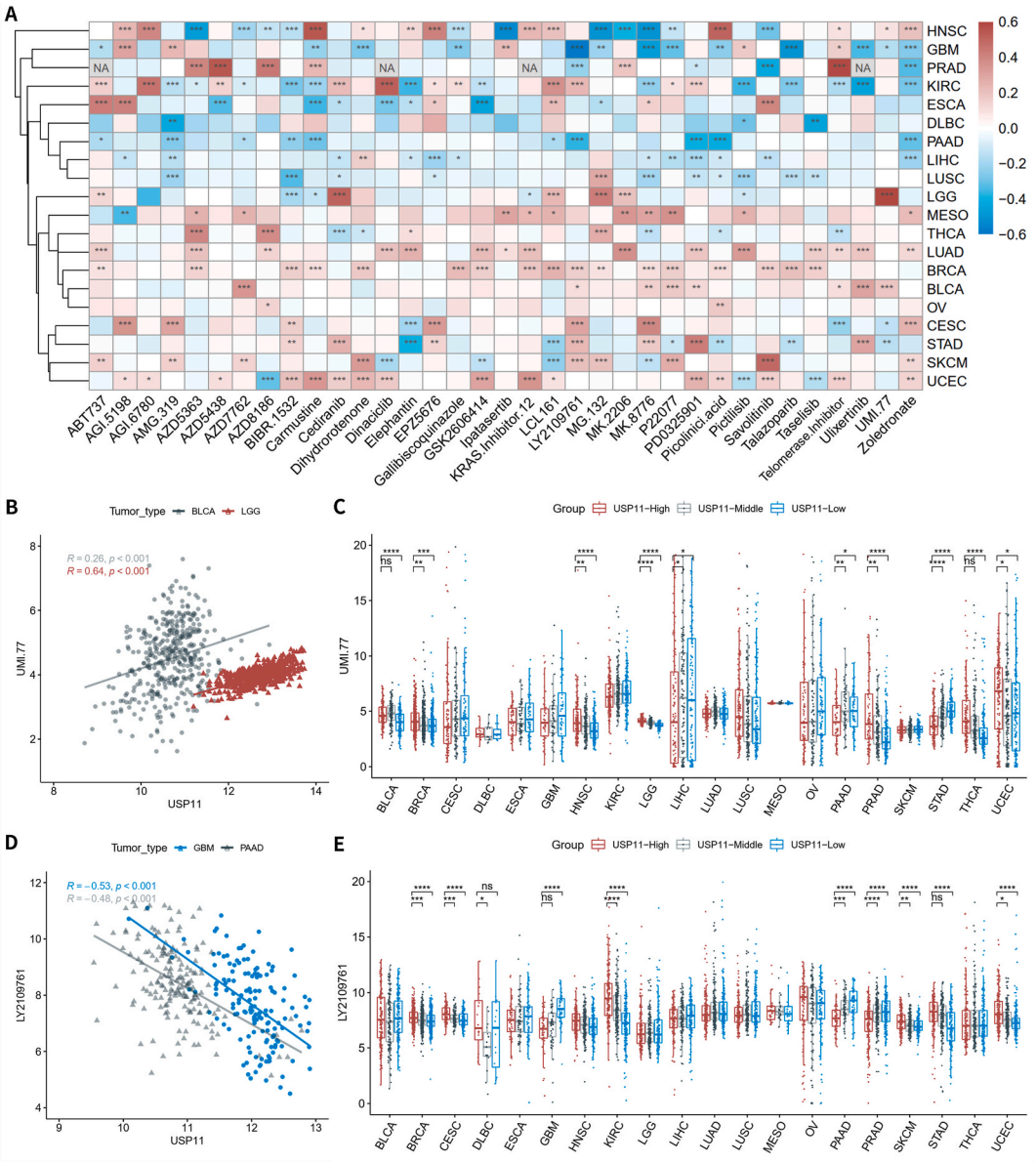

Fig. 8. Potential related drugs. (A) Correlation of *USP11* expression with the sensitivity of thirty-five drugs in pan-cancer by GDSC2 data and ridge regression algorithm. **(B)** The scatter plot of the top positively correlated drug UMI.77 in BLCA. **(C)** Comparisons of the sensitivity of UMI.77 among *USP11* high, middle and low expression groups. **(D)** The scatter plot of the top negatively correlated drug LY2109761 in GBM. **(E)** Comparisons of the sensitivity of LY2109761 among *USP11* high, middle and low expression groups.

in immune infiltration and immunotherapy remains relatively unexplored, insights can be drawn from research on other members of the ubiquitin-specific peptidase family that share homology with *USP11*. Several studies have identified members such as USP3, USP21, USP14, USP25, and USP27X as potential modulators of immune responses through their ability to eliminate K63-linked ubiquitin chains from retinoic acid-inducible gene-I and melanoma differentiation-associated protein 5 [54–58]. Moreover, USP9, USP9X, USP22, and ubiquitin C-terminal hydrolase L1 have been shown to deubiquitinate and stabilize the PD-L1 protein, thereby impacting immune regulation and response [59–61]. Deubiquitination processes have been implicated in various facets of immune regulation, including T cell receptor signaling, T cell differentiation, and immune tolerance, underscoring their significant role in modulating immune responses [62]. Given this growing body of evidence, it is plausible to hypothesize that *USP11* may similarly influence immune responses and potentially hold applications in immunotherapy. In our study, we present novel findings demonstrating that elevated expression of *USP11* correlates with increased immune infiltration of $CD8^+$ T cells and activated NK cells in patients with ESCA, HNSC, LIHC, PRAD, and STAD. Notably, in a cohort of SKCM patients undergoing immunotherapy (phs000452), individuals with high *USP11* expression exhibited a potentially shorter median progression-free survival (PFS) compared to those with

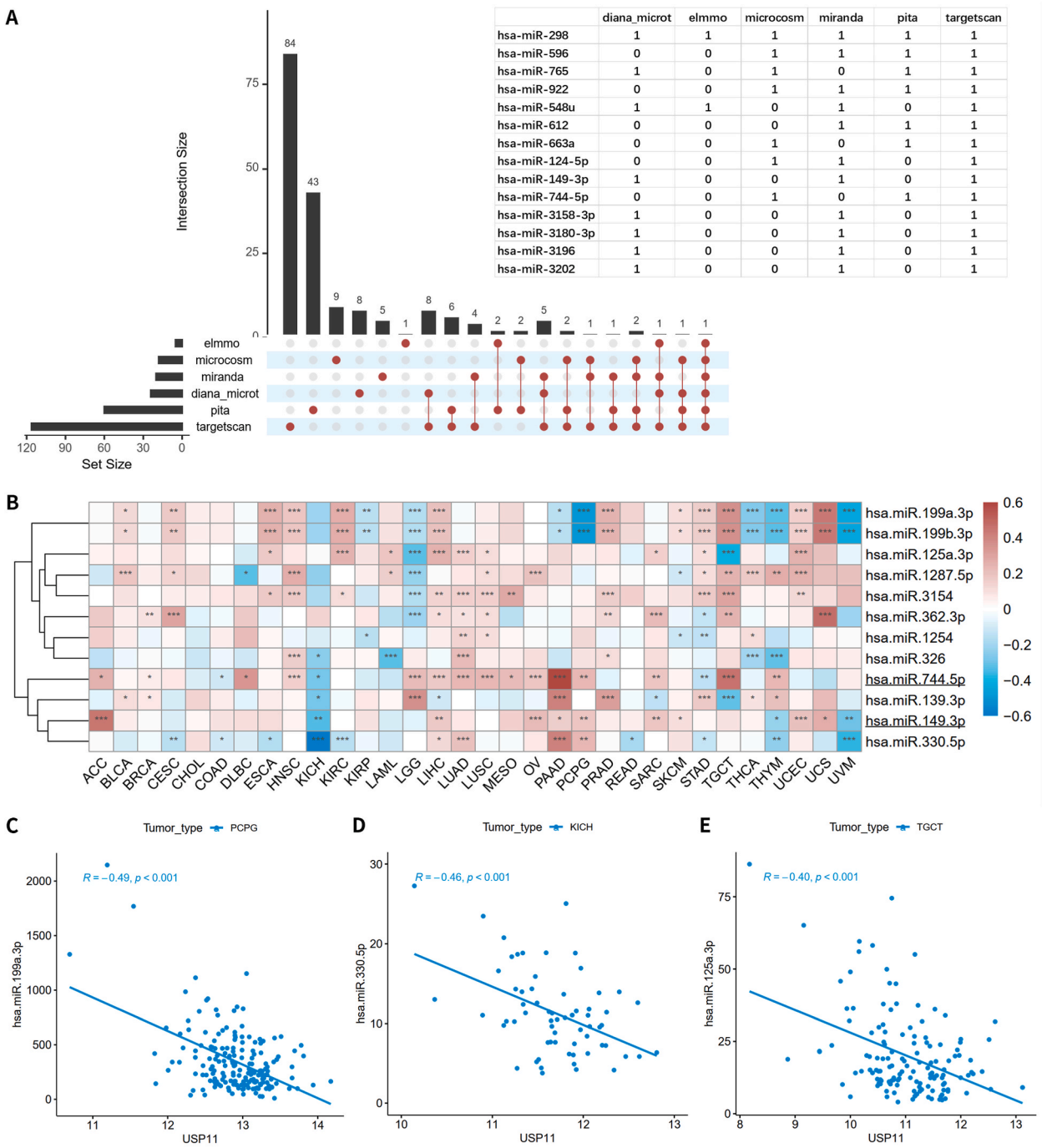

	diana_microt	elmmo	microcosm	miranda	pita	targetscan
hsa-miR-298	1	1	1	1	1	1
hsa-miR-596	0	0	1	1	1	1
hsa-miR-765	1	0	1	0	1	1
hsa-miR-922	0	0	1	1	1	1
hsa-miR-548u	1	1	0	1	0	1
hsa-miR-612	0	0	0	1	1	1
hsa-miR-663a	0	0	1	0	1	1
hsa-miR-124-5p	0	0	1	1	0	1
hsa-miR-149-3p	1	0	0	1	0	1
hsa-miR-744-5p	0	0	1	0	1	1
hsa-miR-3158-3p	1	0	0	1	0	1
hsa-miR-3180-3p	1	0	0	1	0	1
hsa-miR-3196	1	0	0	1	0	1
hsa-miR-3202	1	0	0	1	0	1

Fig. 9. Potential related miRNAs. (A) The upset plot of USP11-targeted miRNAs predicted by six mRNA-miRNA databases, of which miRNAs overlapped in more than three databases was shown in table. **(B)** Expression correlation of *USP11* with miRNAs detected in the TCGA project. **(C–E)** Scatter plots of the top three negatively correlated miRNAs, miR.119a.3p, miR.330.5p and miR.125a.3p.

low *USP11* expression. These observations suggest that *USP11* could serve as a promising biomarker for guiding decisions regarding the suitability of immunotherapy in SKCM patients.

Despite the extensive integration of data from multiple databases regarding the role of *USP11* across various cancers, our study faces several limitations. Firstly, while increased *USP11* expression correlates with improved prognosis in certain tumors, the specific underlying mechanisms remain to be verified. Secondly, the assessment of immune cell infiltration relies on bioinformatic algorithms, potentially introducing systematic biases in immune cell marker analysis. Additionally, all omics data and patient information are

derived from public databases and have not been experimentally validated in clinical settings. Therefore, future investigations should prioritize experimental studies and real-world clinical cohort analyses of *USP11* to elucidate its precise role in tumor immunity and to address these inherent study limitations.

5. Conclusions

In summary, our study utilized bioinformatics approaches to conduct a comprehensive pan-cancer analysis of *USP11*, integrating transcriptomic, genomic, pharmacogenomic, and clinical data. Our findings reveal a significant association between *USP11* expression and both survival prognosis and immune response across various cancer types. Particularly noteworthy is our novel evidence suggesting that *USP11* expression influences the infiltration of $CD8^+$ T cells and NK cells, as well as impacting the progression-free survival of SKCM patients undergoing immunotherapy. Furthermore, we identified potential regulators of *USP11* expression, including small molecule drugs like UMI77 and LY2019761, and miRNAs such as miR-199a-3p and miR-330a-5p. These insights suggest a promising therapeutic strategy involving *USP11* modulators combined with existing checkpoint inhibitors, potentially offering an effective approach to combatting tumors.

Ethical statement

All the data included in the analysis were obtained from public databases without the need of permissions from local ethical committees.

Data availability statement

All raw data used in the present study was downloaded from publicly available repositories. You could download all data included in this study by searching accession numbers from The Cancer Genome Atlas (TCGA) (https://xenabrowser.net/datapages/) and Gene Expression Omnibus (GEO) (https://www.ncbi.nlm.nih.gov/geo/) datasets. The data generated and/or analyzed during our analysis is included in article and supplementary material.

CRediT authorship contribution statement

Lijuan Cui: Writing – review & editing, Writing – original draft, Visualization, Methodology, Data curation, Conceptualization. **Ling Yang:** Methodology, Conceptualization. **Boan Lai:** Visualization, Resources, Formal analysis, Data curation. **Lingzhi Luo:** Visualization, Formal analysis, Data curation. **Haoyue Deng:** Formal analysis, Data curation. **Zhongyi Chen:** Writing – original draft. **Zixing Wang:** Writing – review & editing.

Declaration of competing interest

The authors declare that they have no known competing financial interests or personal relationships that could have appeared to influence the work reported in this paper.

Appendix A. Supplementary data

Supplementary data to this article can be found online at https://doi.org/10.1016/j.heliyon.2024.e34523.

References

[1] H. Ideguchi, A. Ueda, M. Tanaka, J. Yang, T. Tsuji, S. Ohno, E. Hagiwara, A. Aoki, Y. Ishigatsubo, Structural and functional characterization of the USP11 deubiquitinating enzyme, which interacts with the RanGTP-associated protein RanBPM, Biochem. J. 367 (2002) 87–95, https://doi.org/10.1042/BJ20011851.
[2] X. Zhu, R. Ménard, T. Sulea, High incidence of ubiquitin-like domains in human ubiquitin-specific proteases, Proteins: Struct., Funct., Bioinf. 69 (2007) 1–7, https://doi.org/10.1002/prot.21546.
[3] S. Harper, H.E. Gratton, I. Cornaciu, M. Oberer, D.J. Scott, J. Emsley, I. Dreveny, Structure and catalytic regulatory function of ubiquitin specific protease 11 N-terminal and ubiquitin-like domains, Biochemistry 53 (2014) 2966–2978, https://doi.org/10.1021/bi500116x.
[4] S.-Y. Chiang, H.-C. Wu, S.-Y. Lin, H.-Y. Chen, C.-F. Wang, N.-H. Yeh, J.-H. Shih, Y.-S. Huang, H.-C. Kuo, S.-J. Chou, Usp11 controls cortical neurogenesis and neuronal migration through Sox 11 stabilization, Sci. Adv. 7 (2021) eabc6093, https://doi.org/10.1126/sciadv.abc6093.
[5] T. Bouwmeester, A. Bauch, H. Ruffner, P.-O. Angrand, G. Bergamini, K. Croughton, C. Cruciat, D. Eberhard, J. Gagneur, S. Ghidelli, A physical and functional map of the human TNF-α/NF-κB signal transduction pathway, Nat. Cell Biol. 6 (2004) 97–105, https://doi.org/10.1038/ncb1086.
[6] A.C. Schmukle, H. Walczak, No one can whistle a symphony alone–how different ubiquitin linkages cooperate to orchestrate NF-κB activity, J. Cell Sci. 125 (2012) 549–559, https://doi.org/10.1242/jcs.091793.
[7] A. Jacko, L. Nan, S. Li, J. Tan, J. Zhao, D. Kass, Y. Zhao, De-ubiquitinating enzyme, USP11, promotes transforming growth factor β-1 signaling through stabilization of transforming growth factor β receptor II, Cell Death Dis. 7 (2016), https://doi.org/10.1038/cddis.2016.371 e2474-e2474.
[8] E. Zhang, B. Shen, X. Mu, Y. Qin, F. Zhang, Y. Liu, J. Xiao, P. Zhang, C. Wang, M. Tan, Ubiquitin-specific protease 11 (USP11) functions as a tumor suppressor through deubiquitinating and stabilizing VGLL4 protein, Am. J. Cancer Res. 6 (2016) 2901, https://doi.org/10.18632/oncotarget.7581.

[9] A. Spiliotopoulos, L.B. Ferreras, R.M. Densham, S.G. Caulton, B.C. Maddison, J.R. Morris, J.E. Dixon, K.C. Gough, I. Dreveny, Discovery of peptide ligands targeting a specific ubiquitin-like domain–binding site in the deubiquitinase USP11, J. Biol. Chem. 294 (2019) 424–436, https://doi.org/10.1074/jbc.RA118.004469.

[10] A.R. Schoenfeld, S. Apgar, G. Dolios, R. Wang, S.A. Aaronson, BRCA2 is ubiquitinated in vivo and interacts with USP11, a deubiquitinating enzyme that exhibits prosurvival function in the cellular response to DNA damage, Mol. Cell Biol. 24 (2004) 7444–7455, https://doi.org/10.1128/MCB.24.17.7444-7455.2004.

[11] T.D. Wiltshire, C.A. Lovejoy, T. Wang, F. Xia, M.J. O'Connor, D. Cortez, Sensitivity to poly (ADP-ribose) polymerase (PARP) inhibition identifies ubiquitin-specific peptidase 11 (USP11) as a regulator of DNA double-strand break repair, J. Biol. Chem. 285 (2010) 14565–14571, https://doi.org/10.1074/jbc.M110.104745.

[12] M. Sheffer, M.D. Bacolod, O. Zuk, S.F. Giardina, H. Pincas, F. Barany, P.B. Paty, W.L. Gerald, D.A. Notterman, E. Domany, Association of survival and disease progression with chromosomal instability: a genomic exploration of colorectal cancer, Proc. Natl. Acad. Sci. USA 106 (2009) 7131–7136, https://doi.org/10.1073/pnas.0902232106.

[13] S. Peña-Llopis, S. Vega-Rubín-de-Celis, A. Liao, N. Leng, A. Pavía-Jiménez, S. Wang, T. Yamasaki, L. Zhrebker, S. Sivanand, P. Spence, BAP1 loss defines a new class of renal cell carcinoma, Nat. Genet. 44 (2012) 751–759, https://doi.org/10.1038/ng.2323.

[14] H.R. Zhu, X.N. Yu, G.C. Zhang, X. Shi, E. Bilegsaikhan, H.Y. Guo, L.L. Liu, Y. Cai, G.Q. Song, T.T. Liu, Comprehensive analysis of long non-coding RNA-messenger RNA-microRNA co-expression network identifies cell cycle-related lncRNA in hepatocellular carcinoma, Int. J. Mol. Med. 44 (2019) 1844–1854, https://doi.org/10.3892/ijmm.2019.4323.

[15] S. Rousseaux, A. Debernardi, B. Jacquiau, A.-L. Vitte, A. Vesin, H. Nagy-Mignotte, D. Moro-Sibilot, P.-Y. Brichon, S. Lantuejoul, P. Hainaut, Ectopic activation of germline and placental genes identifies aggressive metastasis-prone lung cancers, Sci. Transl. Med. 5 (2013), https://doi.org/10.1126/scitranslmed.3005723, 186ra166-186ra166.

[16] M.T. Landi, T. Dracheva, M. Rotunno, J.D. Figueroa, H. Liu, A. Dasgupta, F.E. Mann, J. Fukuoka, M. Hames, A.W. Bergen, Gene expression signature of cigarette smoking and its role in lung adenocarcinoma development and survival, PLoS One 3 (2008) e1651, https://doi.org/10.1371/journal.pone.0001651.

[17] P.P. Reis, L. Waldron, B. Perez-Ordonez, M. Pintilie, N.N. Galloni, Y. Xuan, N.K. Cervigne, G.C. Warner, A.A. Makitie, C. Simpson, A gene signature in histologically normal surgical margins is predictive of oral carcinoma recurrence, BMC Cancer 11 (2011) 1–11, https://doi.org/10.1186/1471-2407-11-437.

[18] M.V. Yusenko, R.P. Kuiper, T. Boethe, B. Ljungberg, A.G. van Kessel, G. Kovacs, High-resolution DNA copy number and gene expression analyses distinguish chromophobe renal cell carcinomas and renal oncocytomas, BMC Cancer 9 (2009) 1–10, https://doi.org/10.1186/1471-2407-9-152.

[19] O. Kabbarah, C. Nogueira, B. Feng, R.M. Nazarian, M. Bosenberg, M. Wu, K.L. Scott, L.N. Kwong, Y. Xiao, C. Cordon-Cardo, Integrative genome comparison of primary and metastatic melanomas, PLoS One 5 (2010) e10770, https://doi.org/10.1371/journal.pone.0010770.

[20] W.-J. Kim, E.-J. Kim, S.-K. Kim, Y.-J. Kim, Y.-S. Ha, P. Jeong, M.-J. Kim, S.-J. Yun, K.M. Lee, S.-K. Moon, Predictive value of progression-related gene classifier in primary non-muscle invasive bladder cancer, Mol. Cancer 9 (2010) 1–9, https://doi.org/10.1186/1476-4598-9-3.

[21] S. Gulluoglu, E.C. Tuysuz, M. Sahin, A. Kuskucu, C.K. Yaltirik, U. Ture, B. Kucukkaraduman, M.W. Akbar, A.O. Gure, O.F. Bayrak, Simultaneous miRNA and mRNA transcriptome profiling of glioblastoma samples reveals a novel set of OncomiR candidates and their target genes, Brain Res. 1700 (2018) 199–210, https://doi.org/10.1016/j.brainres.2018.08.035.

[22] L. Raskin, D.R. Fullen, T.J. Giordano, D.G. Thomas, M.L. Frohm, K.B. Cha, J. Ahn, B. Mukherjee, T.M. Johnson, S.B. Gruber, Transcriptome profiling identifies HMGA2 as a biomarker of melanoma progression and prognosis, J. Invest. Dermatol. 133 (2013) 2585–2592, https://doi.org/10.1038/jid.2013.197.

[23] R.A. Moffitt, R. Marayati, E.L. Flate, K.E. Volmar, S.G.H. Loeza, K.A. Hoadley, N.U. Rashid, L.A. Williams, S.C. Eaton, A.H. Chung, Virtual microdissection identifies distinct tumor-and stroma-specific subtypes of pancreatic ductal adenocarcinoma, Nat. Genet. 47 (2015) 1168–1178, https://doi.org/10.1038/ng.3398.

[24] K.I. Pappa, A. Polyzos, J. Jacob-Hirsch, N. Amariglio, G.D. Vlachos, D. Loutradis, N.P. Anagnou, Profiling of discrete gynecological cancers reveals novel transcriptional modules and common features shared by other cancer types and embryonic stem cells, PLoS One 10 (2015) e0142229, https://doi.org/10.1371/journal.pone.0142229.

[25] J. Camps, F. Noël, R. Liechti, L. Massenet-Regad, S. Rigade, L. Götz, C. Hoffmann, E. Amblard, M. Saichi, M.M. Ibrahim, Meta-analysis of human cancer single-cell RNA-seq datasets using the IMMUcan database, Cancer Res. 83 (2023) 363–373, https://doi.org/10.1158/0008-5472.CAN-22-0074.

[26] S. Cheng, Z. Li, R. Gao, B. Xing, Y. Gao, Y. Yang, S. Qin, L. Zhang, H. Ouyang, P. Du, A pan-cancer single-cell transcriptional atlas of tumor infiltrating myeloid cells, Cell 184 (2021) 792–809. e723, https://doi.org/10.1016/j.cell.2021.01.010.

[27] T.D. Wu, S. Madireddi, P.E. de Almeida, R. Banchereau, Y.-J.J. Chen, A.S. Chitre, E.Y. Chiang, H. Iftikhar, W.E. O'Gorman, A. Au-Yeung, Peripheral T cell expansion predicts tumour infiltration and clinical response, Nature 579 (2020) 274–278, https://doi.org/10.1038/s41586-020-2056-8.

[28] T.L. Rose, W.H. Weir, G.M. Mayhew, Y. Shibata, P. Eulitt, J.M. Uronis, M. Zhou, M. Nielsen, A.B. Smith, M. Woods, Fibroblast growth factor receptor 3 alterations and response to immune checkpoint inhibition in metastatic urothelial cancer: a real world experience, Br. J. Cancer 125 (2021) 1251–1260, https://doi.org/10.1038/s41416-021-01488-6.

[29] M. Lauss, M. Donia, K. Harbst, R. Andersen, S. Mitra, F. Rosengren, M. Salim, J. Vallon-Christersson, T. Törngren, A. Kvist, Mutational and putative neoantigen load predict clinical benefit of adoptive T cell therapy in melanoma, Nat. Commun. 8 (2017) 1738, https://doi.org/10.1038/s41467-017-01460-0.

[30] R.J. Motzer, P.B. Robbins, T. Powles, L. Albiges, J.B. Haanen, J. Larkin, X.J. Mu, K.A. Ching, M. Uemura, S.K. Pal, Avelumab plus axitinib versus sunitinib in advanced renal cell carcinoma: biomarker analysis of the phase 3 JAVELIN Renal 101 trial, Nat. Med. (N. Y., NY, U. S.) 26 (2020) 1733–1741, https://doi.org/10.1038/s41591-020-1044-8.

[31] D.A. Braun, Y. Hou, Z. Bakouny, M. Ficial, M. Sant'Angelo, J. Forman, P. Ross-Macdonald, A.C. Berger, O.A. Jegede, L. Elagina, Interplay of somatic alterations and immune infiltration modulates response to PD-1 blockade in advanced clear cell renal cell carcinoma, Nat. Med. (N. Y., NY, U. S.) 26 (2020) 909–918, https://doi.org/10.1038/s41591-020-0839-y.

[32] M. Łuksza, N. Riaz, V. Makarov, V.P. Balachandran, M.D. Hellmann, A. Solovyov, N.A. Rizvi, T. Merghoub, A.J. Levine, T.A. Chan, A neoantigen fitness model predicts tumour response to checkpoint blockade immunotherapy, Nature 551 (2017) 517–520, https://doi.org/10.1038/nature24473.

[33] M. Gordon, T. Lumley, M.M. Gordon, Package 'forestplot', Advanced Forest Plot Using 'grid'graphics, The Comprehensive R Archive Network, Vienna, 2019.

[34] T. Therneau, T. Lumley, Package "survival." R Top Doc, 2015, 128, available at:.

[35] A. Kassambara, M. Kosinski, P. Biecek, S. Fabian, survminer: drawing Survival Curves using 'ggplot2, R package version 0. 3 (2017) 1.

[36] Y. Ru, K.J. Kechris, B. Tabakoff, P. Hoffman, R.A. Radcliffe, R. Bowler, S. Mahaffey, S. Rossi, G.A. Calin, L. Bemis, The multiMiR R package and database: integration of microRNA–target interactions along with their disease and drug associations, Nucleic Acids Res. 42 (2014), https://doi.org/10.1093/nar/gku631 e133-e133.

[37] J.R. Conway, A. Lex, N. Gehlenborg, UpSetR: an R package for the visualization of intersecting sets and their properties, Bioinformatics (2017), https://doi.org/10.1093/bioinformatics/btx364.

[38] F.E. Harrell Jr., M.F.E. Harrell Jr., Package 'hmisc', CRAN2018, 2019, pp. 235–236, 2019.

[39] A. Kassambara, M.A. Kassambara, Package 'ggpubr', R package version (2020) 6, 0.1.

[40] R. Kolde, M.R. Kolde, Package 'pheatmap', R Package, vol. 1, 2018.

[41] M.D. Robinson, D.J. McCarthy, G.K. Smyth, edgeR: a Bioconductor package for differential expression analysis of digital gene expression data, Bioinformatics 26 (2010) 139–140, https://doi.org/10.1093/bioinformatics/btp616.

[42] T. Wu, E. Hu, S. Xu, M. Chen, P. Guo, Z. Dai, T. Feng, L. Zhou, W. Tang, L. Zhan, clusterProfiler 4.0: a universal enrichment tool for interpreting omics data, Innovation 2 (2021) 100141, https://doi.org/10.1016/j.xinn.2021.100141.

[43] D. Maeser, R.F. Gruener, R.S. Huang, oncoPredict: an R package for predicting in vivo or cancer patient drug response and biomarkers from cell line screening data, Briefings Bioinf. 22 (2021), https://doi.org/10.1093/bib/bbab260 bbab260.

[44] B. Chen, M.S. Khodadoust, C.L. Liu, A.M. Newman, A.A. Alizadeh, Profiling tumor infiltrating immune cells with CIBERSORT, Cancer Systems Biology: Methods and Protocols 1711 (2018) 243–259, https://doi.org/10.1007/978-1-4939-7493-1_12.

[45] T. Li, J. Fu, Z. Zeng, D. Cohen, J. Li, Q. Chen, B. Li, X.S. Liu, TIMER2. 0 for analysis of tumor-infiltrating immune cells, Nucleic Acids Res. 48 (2020) W509–W514, https://doi.org/10.1093/nar/gkaa407.
[46] H. Sun, B. Ou, S. Zhao, X. Liu, L. Song, X. Liu, R. Wang, Z. Peng, USP11 promotes growth and metastasis of colorectal cancer via PPP1CA-mediated activation of ERK/MAPK signaling pathway, EBioMedicine 48 (2019) 236–247, https://doi.org/10.1016/j.ebiom.2019.08.061.
[47] Y.-Y. Huang, C.-M. Zhang, Y.-B. Dai, J.-G. Lin, N. Lin, Z.-X. Huang, T.-W. Xu, USP11 facilitates colorectal cancer proliferation and metastasis by regulating IGF2BP3 stability, Am. J. Tourism Res. 13 (2021) 480.
[48] R.A. Burkhart, Y. Peng, Z.A. Norris, R.M. Tholey, V.A. Talbott, Q. Liang, Y. Ai, K. Miller, S. Lal, J.A. Cozzitorto, Mitoxantrone targets human ubiquitin-specific peptidase 11 (USP11) and is a potent inhibitor of pancreatic cancer cell survival, Mol. Cancer Res. 11 (2013) 901–911, https://doi.org/10.1158/1541-7786.MCR-12-0699.
[49] D.A. Garcia, C. Baek, M.V. Estrada, T. Tysl, E.J. Bennett, J. Yang, J.T. Chang, USP11 enhances tgfβ-induced epithelial–mesenchymal plasticity and human breast cancer MetastasisTGFβ-induced EMT and metastasis are regulated by USP11, Mol. Cancer Res. 16 (2018) 1172–1184.
[50] L. Dwane, A.E. O'Connor, S. Das, B. Moran, L. Mulrane, A. Pinto-Fernandez, E. Ward, A.M. Blümel, B.L. Cavanagh, B. Mooney, A functional genomic screen identifies the deubiquitinase USP11 as a novel transcriptional regulator of ERα in breast CancerThe role of USP11 in ERα function in breast cancer, Cancer Res. 80 (2020) 5076–5088, https://doi.org/10.1158/0008-5472.CAN-20-0214.
[51] S. Zhang, C. Xie, H. Li, K. Zhang, J. Li, X. Wang, Z. Yin, Ubiquitin-specific protease 11 serves as a marker of poor prognosis and promotes metastasis in hepatocellular carcinoma, Lab. Invest. 98 (2018) 883–894, https://doi.org/10.1038/s41374-018-0050-7.
[52] C. Zhang, C. Xie, X. Wang, Y. Huang, S. Gao, J. Lu, Y. Lu, S. Zhang, Aberrant USP11 expression regulates NF90 to promote proliferation and metastasis in hepatocellular carcinoma, Am. J. Cancer Res. 10 (2020) 1416.
[53] P. Feng, L. Li, J. Dai, L. Zhou, J. Liu, J. Zhao, X. Li, N. Ling, S. Qiu, L. Zhang, The regulation of NONO by USP11 via deubiquitination is linked to the proliferation of melanoma cells, J. Cell Mol. Med. 25 (2021) 1507–1517, https://doi.org/10.1111/jcmm.16243.
[54] J. Cui, Y. Song, Y. Li, Q. Zhu, P. Tan, Y. Qin, H.Y. Wang, R.-F. Wang, USP3 inhibits type I interferon signaling by deubiquitinating RIG-I-like receptors, Cell Res. 24 (2014) 400–416, https://doi.org/10.1038/cr.2013.170.
[55] H. Li, Z. Zhao, J. Ling, L. Pan, X. Zhao, H. Zhu, J. Yu, B. Xie, J. Shen, W. Chen, USP14 promotes K63-linked RIG-I deubiquitination and suppresses antiviral immune responses, Eur. J. Immunol. 49 (2019) 42–53, https://doi.org/10.1002/eji.201847603.
[56] Y. Fan, R. Mao, Y. Yu, S. Liu, Z. Shi, J. Cheng, H. Zhang, L. An, Y. Zhao, X. Xu, USP21 negatively regulates antiviral response by acting as a RIG-I deubiquitinase, J. Exp. Med. 211 (2014) 313–328, https://doi.org/10.1084/jem.20122844.
[57] H. Zhong, D. Wang, L. Fang, H. Zhang, R. Luo, M. Shang, C. Ouyang, H. Ouyang, H. Chen, S. Xiao, Ubiquitin-specific proteases 25 negatively regulates virus-induced type I interferon signaling, PLoS One 8 (2013) e80976, https://doi.org/10.1371/journal.pone.0080976.
[58] X. Tao, B. Chu, D. Xin, L. Li, Q. Sun, USP27X negatively regulates antiviral signaling by deubiquitinating RIG-I, PLoS Pathog. 16 (2020) e1008293, https://doi.org/10.1371/journal.ppat.1008293.
[59] W. Jingjing, G. Wenzheng, W. Donghua, H. Guangyu, Z. Aiping, W. Wenjuan, Deubiquitination and stabilization of programmed cell death ligand 1 by ubiquitin-specific peptidase 9, X-linked in oral squamous cell carcinoma, Cancer Med. 7 (2018) 4004–4011, https://doi.org/10.1002/cam4.1675.
[60] R. Mao, X. Tan, Y. Xiao, X. Wang, Z. Wei, J. Wang, X. Wang, H. Zhou, L. Zhang, Y. Shi, Ubiquitin C-terminal hydrolase L1 promotes expression of programmed cell death-ligand 1 in non-small-cell lung cancer cells, Cancer Sci. 111 (2020) 3174–3183, https://doi.org/10.1111/cas.14529.
[61] X. Huang, Q. Zhang, Y. Lou, J. Wang, X. Zhao, L. Wang, X. Zhang, S. Li, Y. Zhao, Q. Chen, USP22 deubiquitinates CD274 to suppress anticancer immunityUSP22 is a deubiquitinase of CD274, Cancer Immunol. Res. 7 (2019) 1580–1590, https://doi.org/10.1158/2326-6066.CIR-18-0910.
[62] P. Zeng, J. Ma, R. Yang, Y.-C. Liu, Immune regulation by ubiquitin tagging as checkpoint code, Emerging Concepts Targeting Immune Checkpoints in Cancer and Autoimmunity (2017) 215–248, https://doi.org/10.1007/82_2017_64.